Traveling Waves in a Ring of Three Inhibitory Coupled Model Neurons

Susanne Still [a,1] and Gwendal Le Masson [b]

[a] *Institute of Neuroinformatics, ETH and University Zürich, Switzerland*

[b] *INSERM, U378, Institute Francois Magendie, Bordeaux, France*

Abstract

The pyloric network of the stomatogastric ganglion of the lobster generates motor patterns with specific phase-lags between single neurons. This network inspired us to investigate a simplified model consisting of three mono-directionally coupled Morris-Lecar oscillators. We have systematically analyzed the high-dimensional space of the synaptic parameters and identified parameter combinations which lead to biologically plausible phase-lags that exist even in a network with identical cells in the absence of an intrinsic burster. The dependence of the phase lags on the synaptic parameters was also explored.

Key words: Morris-Lecar, coupled oscillators, ring network

1 Introduction

A network with three model neurons, coupled with mono-directional inhibition could, in principal, be used to control various asynchronous movement sequences by producing patterns with different phase lags. This makes its behavior interesting with respect to biological as well as artificial movement control. A related system is the pyloric network in the stomatogastric (STG) ganglion of the lobster (*Jasus lalandii*), which consists of 14 STG neurons and controls rhythmic contractions of the pyloric region of the foregut (fig. 1A, B) (2; 3). The dilator group consists of pyloric dilator neurons (PD) and an anterior burster (AB). The anterior constrictor group consists of a lateral pyloric neuron (LP) and the posterior constrictor group is formed by pyloric neurons (PY). The neurons within each group tend to be synchronously active due to

[1] Supported by the CSEM and the SNSF SPP.

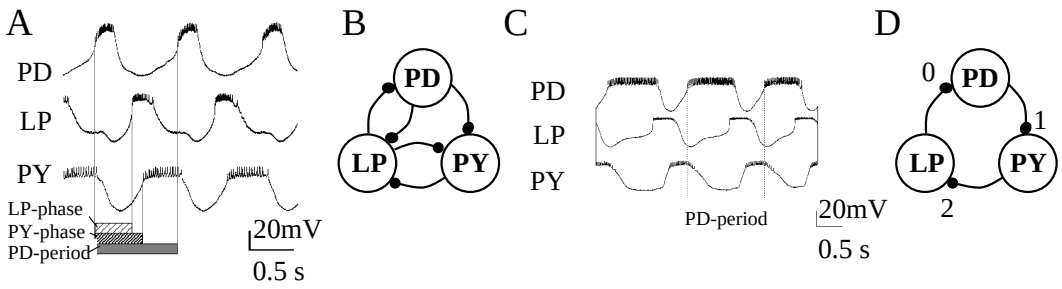

Fig. 1. The pyloric network and the hybrid network. A) Typical recording from the neurons of the pyloric network showing the voltages of the three cell groups PD, LP and PY as a function of time (from (3)). LP- and PY-phase lags are indicated by the bars at the bottom. B) Sketch of the corresponding network architecture. C) Typical recording from the hybrid network (3), showing the voltages of the cell groups as a function of time. D) Network architecture corresponding to C. In our model, the PD cell is numbered 0, the PY cell 1 and the LP cell 2 (see fig. 1D).

electric coupling. The synapses are inhibitory. This network generates oscillations which are characterized by the phase lags between the different groups, defined as: x-phase=(time between onset of PD-burst and x-burst)/(pyloric period), where x stands for either LP or PY and the pyloric period is the time between onsets of two adjacent PD-bursts (fig. 1A). Typical values are: LP-phase=0.4, PY-phase=0.7 and pyloric frequency=1 Hz (4). A hybrid network was constructed by replacing PD with a model neuron, implemented on a computer and interfaced with artificial synapses (3). The network architecture was reduced to a ring of mono-directionally coupled neurons (fig. 1C, D). The typical phase lags of the hybrid network are 0.55 to 0.6 for LP and 0.76 to 0.8 for PY. We consider a model (fig. 1D) of the same architecture that additionally produces patterns like the pyloric network. Examination of the synaptic properties of this model enabled us to investigate under which circumstances the model can produce a pyloric pattern and furthermore to find out how the phase lags of the asynchronous traveling waves that the model produces depend on the synaptic parameters.

2 Methods

Each neuron is modeled by the reduced Morris-Lecar equations (Appendix). They are a set of two differential equations originally formulated to model the barnacle giant muscle fiber (5) and represent an abstraction rather than a detailed biophysical model of the STG neuron groups. The voltage variable V (Appendix) models the envelope of the spiking. Therefore an oscillation of V indicates a burst. This simplification is justified, because the envelope expresses the features of the pattern which are relevant for our purposes. Different intrinsic properties of the uncoupled neurons are captured by the model.

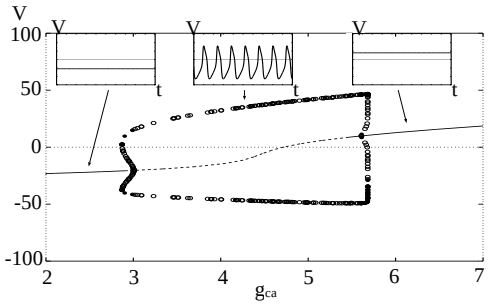

Fig. 2. Bifurcation diagram of Morris Lecar model neuron. V vs. maximum calcium conductance g_{ca}. A stable steady state (solid part of line) becomes unstable (dashed part of line) for increased g_{ca}. Hopf bifurcation occurs and leads to periodic solutions. Circles indicate the maximum and minimum voltage of these oscillations. There is a stable steady state for large g_{ca}. The insets show the cell voltage as a function of time for examples in three different regimes (arrows). Tonic spiking is indicated by a constant V above the firing threshold (right), bursting behavior is given by oscillations of V (middle). A silent cell would be expressed by a constant voltage below threshold (left).

(fig. 2). The synaptic coupling is modeled by a voltage and time-dependent current (Appendix). The maximal synaptic conductances (g_{syn}) and the synaptic time constants (τ_s) of each cell give rise to the six-dimensional parameter space that was investigated to explore the effect of the synaptic coupling on the phase lags.

3 Results

First, the PD-cell is modeled as an intrinsic burster, while the other two cells are modeled as tonic firing when uncoupled and the synapses are not identical (fig. 3.1-3 and figs. 4, 5). The model reproduces a pattern with phase lags that match the ones of the hybrid network (fig. 3.1). Stable solutions with such phase lags occur in an extended region in parameter space (fig. 4). In this configuration the network can produce a variety of asynchronous traveling waves, the phase lags of which depend on the synaptic parameters. Typical one-dimensional slices through the six-dimensional parameter space are shown in fig. 5. The phase lags are smooth functions of the synaptic parameters. This network also produces patterns with phase lags like the ones typically measured in the pyloric network (fig. 3.2). Synchronous solutions can be found as well (fig. 3.3). These are an interesting feature of the network. The bursting cell (PD) drives the network into synchronization, if the inhibition to PD is small ($g_{syn,0} = 0.8$), and the other two cells are strongly inhibited ($g_{syn,1} = g_{syn,2} = 4.8$). With identical synapses the network can produce neither the typical phase lags of the pyloric network nor those of the hybrid

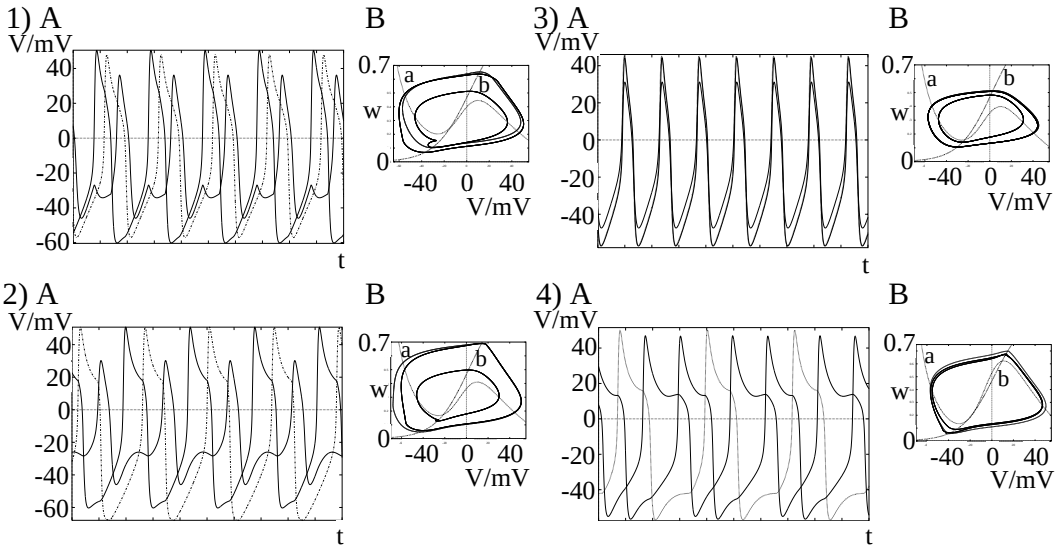

Fig. 3. Examples of patterns produced by the model. 1) Hybrid network pattern. LP-phase=0.59, PY-phase=0.78. 2) Pyloric network pattern. LP-phase=0.4, PY-phase=0.7. 3) Synchronous activity. 4) Pyloric network pattern by identical (tonic) neurons. LP-phase=0.4, PY-phase=0.71. A) Voltage traces of the three cells as a function of time after the network has settled into a stable state. PD, thin, LP, thick and PY, dotted line. B) Phase plane portrait (6; 7). The trajectories for the three cells are shown over a period of 1000 s. Notice that they lie on limit cycles. Dashed lines show the nullclines $\dot{V} = 0$ (a) and $\dot{w} = 0$ (b).

network in the investigated parameter space (fig. 6). The parameter combinations for which the LP-phase ≥ 0.4 and the PY-phase is maximum (0.66) do not overlap (fig. 6, indicated by outlined areas), and the PY-phase does not attain a value of 0.7. The network with identical cells (without an intrinsic burster) can produce solutions that exhibit traveling waves with phase lags like the ones found in the pyloric network, if the synapses are not identical (fig. 3.4).

4 Conclusion

A ring of three model neurons, coupled with mono-directional inhibition produces traveling waves with phase lags typical of those measured in the pyloric network of the lobster STG, only when the synaptic coupling is not identical. This is independent of whether or not the ring contains an intrinsically bursting cell. In the presence of an intrinsically bursting cell and non-identical synapses the phase lags of the asynchronous traveling waves depend smoothly on the parameters g_{syn} and τ_s of each synapse in an investigated regime. Synchronous activity can occur in the model. Similar networks could be used to

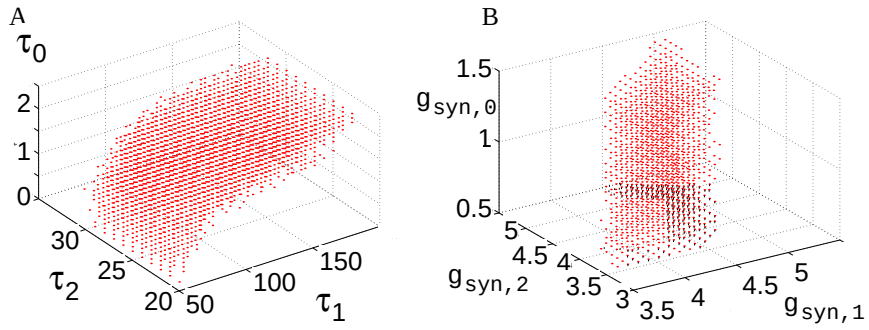

Fig. 4. Oscillations of the model with phase-lags that match those of the hybrid network (LP-phase between 0.55 and 0.6, PY-phase between 0.76 and 0.8) Location (indicated by dots) in the parameter spaces of A) the synaptic time constants, $\tau_{s,i}$, and B) the maximal synaptic conductances, $g_{syn,i}$.

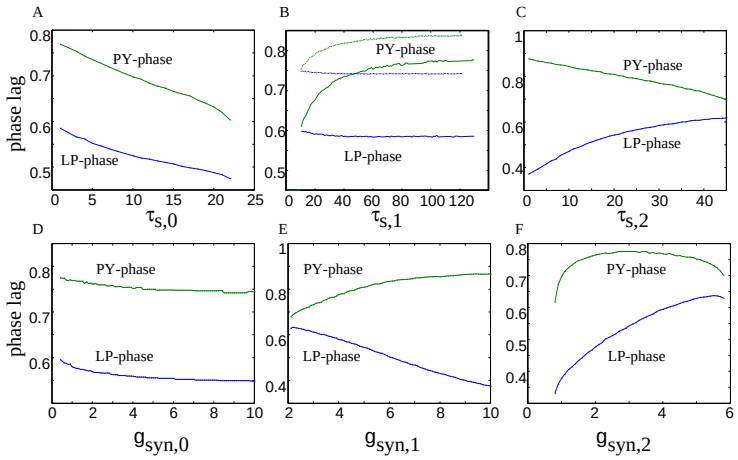

Fig. 5. LP-phase and PY-phase shown as functions of the synaptic time constant of A) PD cell ($\tau_{s,0}$), B) PY cell ($\tau_{s,1}$) C) LP cell ($\tau_{s,2}$) and of the maximal synaptic conductance of D) PD cell ($g_{syn,0}$), E) PY cell ($g_{syn,1}$), F) LP cell ($g_{syn,2}$).

control various rhythmic asynchronous sequences for locomotion (1). A possible application for the network discussed here could be to control the relative timing of three joints in robotic legs during walking.

5 Appendix

$$\dot{V} = \frac{1}{C}(I_{ext} + g_l(V_l - V) + g_k w(V_k - V) + g_{ca} m_\infty (V_{ca} - V) + g_{syn} s(V_{syn} - V))$$

$$\dot{w} = \phi(\cosh \frac{V - V_{p3}}{2V_{p4}})(w_\infty - w) \text{ with } w_\infty = \frac{1}{2}(1 + \tanh \frac{V - V_{p3}}{V_{p4}})$$

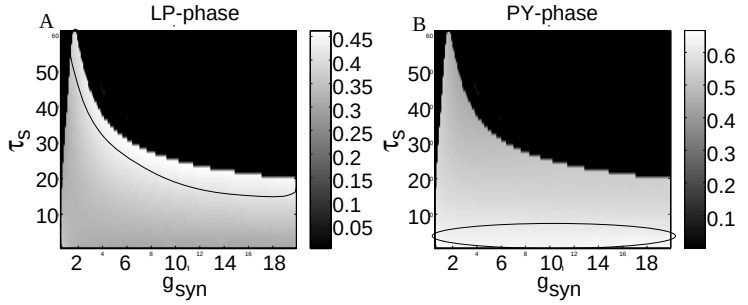

Fig. 6. Phase lags as a function of the maximal synaptic conductances ($g_{syn} = g_{syn,i}$) and the synaptic time constants ($\tau_s = \tau_{s,i}$) for identical synapses ($i = 0, 1, 2$). $g_{ca,0} = 4$, $g_{ca,1,2} = 6.5$. A) LP-phase. B) PY-phase. The magnitude of the phase-lags is coded with different shades of gray as indicated by bars. The black regime (value=0) represents regimes in which not every cell bursts once per network period, solutions that are not considered here. The values of LP- and PY-phase for a given combination of the two parameters can be read out in both diagrams at the same place. Outlined regions are referred to in the text.

$\dot{s} = (s_\infty - s)/\tau_s$ with $s_\infty = \frac{1}{2}(1 + \tanh \frac{V_{pre} - V_{th}}{V_{slope}})$; $m_\infty = \frac{1}{2}(1 + \tanh \frac{V - V_{p1}}{V_{p2}})$

where: C = capacitance; V = membrane voltage; V_{pre} = presynaptic membrane voltage; I_{ext} = external current; $g_l, g_k, g_{ca}, g_{syn}$ = maximal conductances of the leak, K^+, Ca^{2+} and synaptic current; $V_l, V_k, V_{ca}, V_{syn}$ = reversal potentials for these conductances; $m_\infty, w_\infty, s_\infty$ = fraction of open Ca^{2+}, K^+ and synaptic channels at steady state; w and s = fraction of open K^+ and synaptic channels; ϕ = minimum rate constant for K^+ channel opening; V_{p1}, V_{p3}, V_{th} = voltage at which half of the Ca^{2+}, K^+ and synaptic channels are open at steady-state; $V_{p2}, V_{p4}, V_{slope}$ = reciprocal of the slope of voltage dependency of the fraction of open Ca^{2+}, K^+ and synaptic channels at steady-state; τ_s = synaptic time constant (7). Parameters: For tonic spiking: $I_{ext} = 120, g_l = 1.8, V_l = -60, g_k = 8, V_k = -84, g_{ca} = 6.5, V_{ca} = 120, C = 2, V_{p1} = -1.2, V_{p2} = 18, V_{p3} = 2, V_{p4} = 30, \phi = 0.04, V_{syn} = -84, V_{th} = 0, V_{slope} = 1, g_{syn}$ and τ_s as indicated below. For bursting: The same, except for $g_{ca} = 4$. Parameters are numbered with corresponding cell numbers. Parameters in fig. 3: 1) $\tau_{s,0}$=1, $\tau_{s,1}$=90, $\tau_{s,2}$=30, $g_{syn,0}$=0.8, $g_{syn,1}$=3.9, $g_{syn,2}$=3.8. 2) $\tau_{s,0..2}$=28, $g_{syn,0}$=0.8, $g_{syn,1}$=12, $g_{syn,2}$=4. 3) $\tau_{s,0..2}$=28, $g_{syn,0}$=0.8, $g_{syn,1}$=4.8, $g_{syn,2}$=4.8. 4) $\tau_{s,0}$=91, $\tau_{s,1}$=31, $\tau_{s,0}$=71, $g_{syn,0}$=2, $g_{syn,1}$=2, $g_{syn,2}$=3. Constant parameters in figs. 4 and 5 are as in fig. 3.1. Units: Voltage in mV, conductance in muS/cm^2, current in nA/cm^2 and capacitance in $\mu F/cm^2$. Simulations were carried out with XPP (6) and a C program, written by us.

References

[1] C. C. Canavier et al., Phase response characteristics of model neurons determine which patterns are expressed in a ring circuit model of gait

generation. *Biol. Cybern.* **77** (1997) 367-380

[2] R. M. Harris-Warrick, E. Marder, A. I. Selverston, and M. Moulins, Eds. *Dynamic Biological Networks: The Stomatogastric Nervous System.* (Cambridge, MA. MIT Press, 1992).

[3] G. LeMasson, S. LeMasson, M. Moulins, From Conductances To Neural Network Properties: Analysis Of Simple Circuits Using The Hybrid Network Method. *Prog. Biophys. Molec. Biol.* **64** (1995) No.2/3, 201-220.

[4] J. P. Miller, Pyloric Mechanisms. in: A. I. Selverston and M. Moulins, eds. *The Crustacean Stomatogastric System* (Springer Verlag, Berlin, 1987) 109-136.

[5] C. Morris, H. Lecar, Voltage oscillations in the barnacle giant muscle fiber. *Biophys. J.* **35** (1981) 193-213

[6] J. Rinzel, B. Ermentrout, Analysis of Neural Excitability and Oscillations, in: C. Koch and I. Segev, Eds. *Methods in Neuronal Modeling* (2nd ed. MIT Press, 1998).

[7] F. K. Skinner, N. Kopell, E. Marder, Mechanisms for Oscillation and Frequency Control in Reciprocally Inhibitory Model Neural Networks. *J. Comput. Neurosci.* **1** (1994) 69-87